Science of the Total Environment 819 (2022) 153182

Contents lists available at ScienceDirect

Science of the Total Environment

journal homepage: www.elsevier.com/locate/scitotenv

Land-use changes and precipitation cycles to understand hydrodynamic responses in semiarid Mediterranean karstic watersheds

Teresa Palacios-Cabrera [a], Javier Valdes-Abellan [b,c,*], Antonio Jodar-Abellan [d,c], Jesús Rodrigo-Comino [d]

[a] Faculty of Geology, Mines, Petroleum and Environmental Engineering, Central University of Ecuador, Ecuador
[b] Department of Civil Engineering, University of Alicante, Spain
[c] University Institute of Water and Environmental Sciences, University of Alicante, Spain
[d] Departamento de Análisis Geográfico Regional y Geografía Física, Facultad de Filosofía y Letras, Campus Universitario de Cartuja, University of Granada, 18071 Granada, Spain

HIGHLIGHTS

- Land-use changes in Mediterranean arid karstic areas were assessed.
- Hydrological responses to changes in rainfall patterns were assessed using wavelet analysis.
- Surface available water would decrease during higher occurrences of peak flow events.
- It was shown that the new ANSE index improved the goodness-of-fit measurement for these areas.
- Also, we demonstrated that the HEC-HMS model is suitable to assess water issues of karstic areas.

GRAPHICAL ABSTRACT

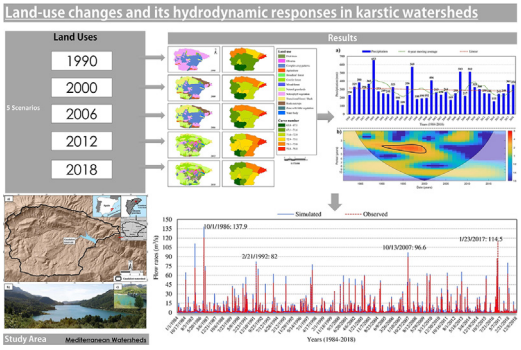

ARTICLE INFO

Article history:
Received 9 August 2021
Received in revised form 11 January 2022
Accepted 12 January 2022
Available online 16 January 2022

Editor: Christian Herrera

Keywords:
Land-use changes
Agricultural abandonment
CN number
Precipitation trends
Runoff prediction
Hydrological modeling

ABSTRACT

Non-planned agricultural land abandonment is affecting natural hydrological processes. This is especially relevant in vulnerable arid karstic watersheds, where water resources are scarce but vital for sustaining natural ecosystems and human settlements. However, studies assessing the spatiotemporal evolution of the hydrological responses considering land-use changes and precipitation cycles for long periods are rare in karstic environments. In this research, we selected a representative karstic watershed in a Mediterranean semiarid domain, since in this belt, karst environments are prone to land degradation processes due to human impacts. Geographic Information Systems-based tools and hydrological modeling considering daily time steps were combined with temporal analysis of climate variables (wavelet analysis) to demonstrate possible interactions and vulnerable responses. Observed daily flow data were used to calibrate/validate these hydrological models by applying statistic indicators such as the NSE efficiency and a self-developed index (the ANSE index). This new index could enhance goodness-of-fit measurements obtained with traditional statistics during the model optimization. We hypothesize that this is key to adding new inputs to this research line. Our results revealed that: i) changes in the type of sclerophyllous vegetation (*Quercus calliprinos*, *ilex*, *rotundifolia*, *suber*, etc.) from 81.5% during the initial stage (1990) to natural grasslands by 81.6% (2018); and, ii) decreases in agricultural areas (crops) by approximately 60% and their transformation into coniferous forests, rock outcrops, sparsely natural grasslands, etc. in the same period. Consequently, increases in the curve number (CN) rates were identified as a result of land abandonment. As a result, an increase in peak flow events jointly with a relevant decrease of the average flow rates (water scarcity) in the watershed was predicted by the HEC-HMS model and verified through the observed data. This research provides useful information about the effects of anthropogenic changes in the hydrodynamic

* Corresponding author at: Department of Civil Engineering, University of Alicante, Spain.
E-mail address: javier.valdes@ua.es (J. Valdes-Abellan).

http://dx.doi.org/10.1016/j.scitotenv.2022.153182

behaviour of karstic watersheds and water resource impacts, especially key in water-scarce areas that depict important hazards for the water supply of related populations and natural ecosystems.

1. Introduction

Water resources management must follow a holistic perspective that includes multiple hydrological components interacting among them (Abbaspour et al., 2017; Boongaling et al., 2018; Ricart and Rico, 2019; Buonocore et al., 2021). However, human activities introduce changes in the natural environmental systems to date, with non-well-known impacts such as drastic land-use changes or the over-exploitation of natural resources such as water, soils, etc. (Aburas et al., 2019; Assefa et al., 2020). Particularly, land-use changes are producing variations in the hydrological response with irreparable modification of the water cycle and increases in the maximum flow peaks during runoff events (Camarasa-Belmonte, 2016; Alonso-Sarría et al., 2016; Csáki et al., 2020; Sánchez-Galiano et al., 2017; Pardo et al., 2020). Nowadays, the application of remote sensing techniques (RS) and Geographical Information Systems (GIS) has propelled Earth observations, improving the identification and mapping of land use and respective changes (Petchprayoon et al., 2010; Nayeb-Yazdi et al., 2021; Đukic and Erić, 2021). Among those hydrological components involved after drastic land-use changes, the most relevant ones to achieve sustainable water management are related to the assessment of floods and water availability, since the variation of both factors could lead to significant modifications on the ecosystem services and human security (Jodar-Abellan et al., 2019; Lasanta et al., 2021).

Over the world, and especially across the Mediterranean belt, several authors have reported that river basin systems are being affected by high human pressures and immediate solutions are needed (Gassman et al., 2007; García and Cutillas, 2014; Cerdà et al., 2021a and Cerdà et al., 2021b). Deforestation, land fragmentation, wetland cultivation or rapid urbanization are some examples of water catchment degradation, resulting in reduced baseflow, drying up of small streams and water wells, floods and water shortages (Andrade and Szlafsztein, 2018; Alonso-Sarría et al., 2016; Gao et al., 2020). Improving the knowledge of the links between land-use and land cover changes (LULC) and the hydrological response is vital for developing proper plans to manage water resources correctly and reduce flood risks. However, this is a difficult task since these changes may present a high spatiotemporal variability (Valdes-Abellan et al., 2020; Tohuami et al., 2013; Buonocore et al., 2021). Additionally, observed changes in the precipitation trends employing volume, number of events and intensity would threaten Mediterranean societies in future decades in these types of catchments (Valdes-Abellan et al., 2017).

Since the 2000s, several studies are trying to demonstrate the correlation between rainfall intensity, unexpected hydrological responses and land-use changes (Abbaspour et al., 2017; Hu et al., 2021; Gassman et al., 2007). In the Mediterranean area, high-intensity convective storms and the presence of complex topography close to the coastal areas constitute additional factors to be considered (Amengual et al., 2015; Ballesteros et al., 2018). This is highly remarkable for urban areas, where alterations in the albedo effect create heat islands and greenhouse emissions among others, varying the water balances and surface energy (Jodar-Abellan et al., 2019; Elaji and Ji, 2020; Senciales-González et al., 2020). The consequences of this situation have been widely identified in many studies in the most affected provinces of Eastern and Southeastern Spain such as Almeria, Murcia or Alicante (Molina-Sanchis et al., 2016; Amengual et al., 2015; Conesa-García et al., 2017; Hooke, 2016).

`To date, the main challenge is to effectively approach the potential land use modification and the corresponding storm runoff patterns (Peña-Angulo et al., 2021). Recent studies adopted past and present land-use cover conditions to project extreme future scenarios, which can be used as inputs to design new hydrological models (García-Ruiz and Lana-Renault, 2011; Boongaling et al., 2018; Rafiei-Emam et al., 2016).

Among different approaches, GIS-based hydrological modeling systems are becoming increasingly relevant tools because of their ability to handle spatial variations at the basin scale with a huge number of physiographic inputs (Nguyen et al., 2020; Senent-Aparicio et al., 2020; Jodar-Abellan et al., 2018). Several models have been developed such as SWAT (Arnold et al., 1998; Arnold et al., 2012), MODFLOW (Mcdonald and Harbaugh, 1984) or HEC-RAS (Brunner and Bonner, 1994; Ferreira et al., 2020). Most of them are integrated into a GIS framework and have demonstrated efficiently the ability to import spatiotemporal attributes. This implementation is more common in detrital environments, while modeling hydrological processes in other conditions, such as karstic areas, remains limited currently (e.g. Moriasi et al., 2007; Candela et al., 2012; Azmat et al., 2018; Robineau et al., 2018; Ollivier et al., 2020; Đukic and Erić, 2021; Chen et al., 2021). The Hydrologic Engineering Center-Hydrologic Modeling System (HEC-HMS) model (Charley et al., 1995; Fleming and Brauer, 2018) is another appropriate well-known alternative for analysing the hydrological response sequentially and to examine the hydrological impact of the identified land-use changes (Gao et al., 2020; Fleming and Brauer, 2018; Mahmood and Jia, 2019). It allows simulating the rainfall-runoff and routing processes (Charley et al., 1995; Hu and Shrestha, 2020). HMS is a semi-distributed model that allows the division of the catchment into multiple sub-basins, taking into account individual responses. Moreover, it can simulate events in both short- and long-terms, adopting common methods with simplified parameters to operate (Koneti et al., 2018; Khoi, 2016; Fleming and Brauer, 2018). HMS can be run with different computational time steps, according to the aim of the simulation and the representativeness of the short-time events in the study area (Jeong et al., 2010; Charley et al., 1995; Koneti et al., 2018; Azmat et al., 2018). HMS has been widely applied in uncalibrated basins with generally accurate results (Candela et al., 2012; Boongaling et al., 2018; Elaji and Ji, 2020; Đukic and Erić, 2021). To the best of our knowledge, however, it was not tested in arid karstic environments affected by drastic land-use and land cover changes.

Therefore, the main aim of this research is to identify the impacts of the anthropic action using change of land-uses on the hydrological processes considering precipitation trends. We will try to decipher how these changes may impact the curve number rates, surface runoff, and stream discharges. To achieve this goal, a karstic Mediterranean watershed located in Southeastern Spain was selected using a long-term dataset from 1990 to 2018. We hypothesize that our results could help to design integral watershed management plans, reproducible for similar areas over the world with similar environmental characteristics.

2. Materials and methods

2.1. Study area

The research was conducted in the Guadalest karstic watershed, within the Jucar river basin district (DPA-IGME, 2015; Fig. 1), located in the province of Alicante (SE Spain). It flows from the confluence of the Fabara and Beniardá ravines at the foothill of the Serella mountain range. The main elevations reach up to 1400 m.a.s.l. and are at a distance of less than 20 km from the coastal line. The watershed ends in the Guadalest reservoir (Fig. 2) at an elevation of 363 m.a.s.l. The watershed depicts an area of 62 km^2 with steep slopes and a reservoir presenting a capacity of 13 hm^3 and a maximum water surface of 86 ha (CHJ, 2013). The area is classified as a semi-arid Mediterranean climate, with averaging the annual temperature of 18 °C and total annual precipitation from 250 to 450 mm (Valdes-

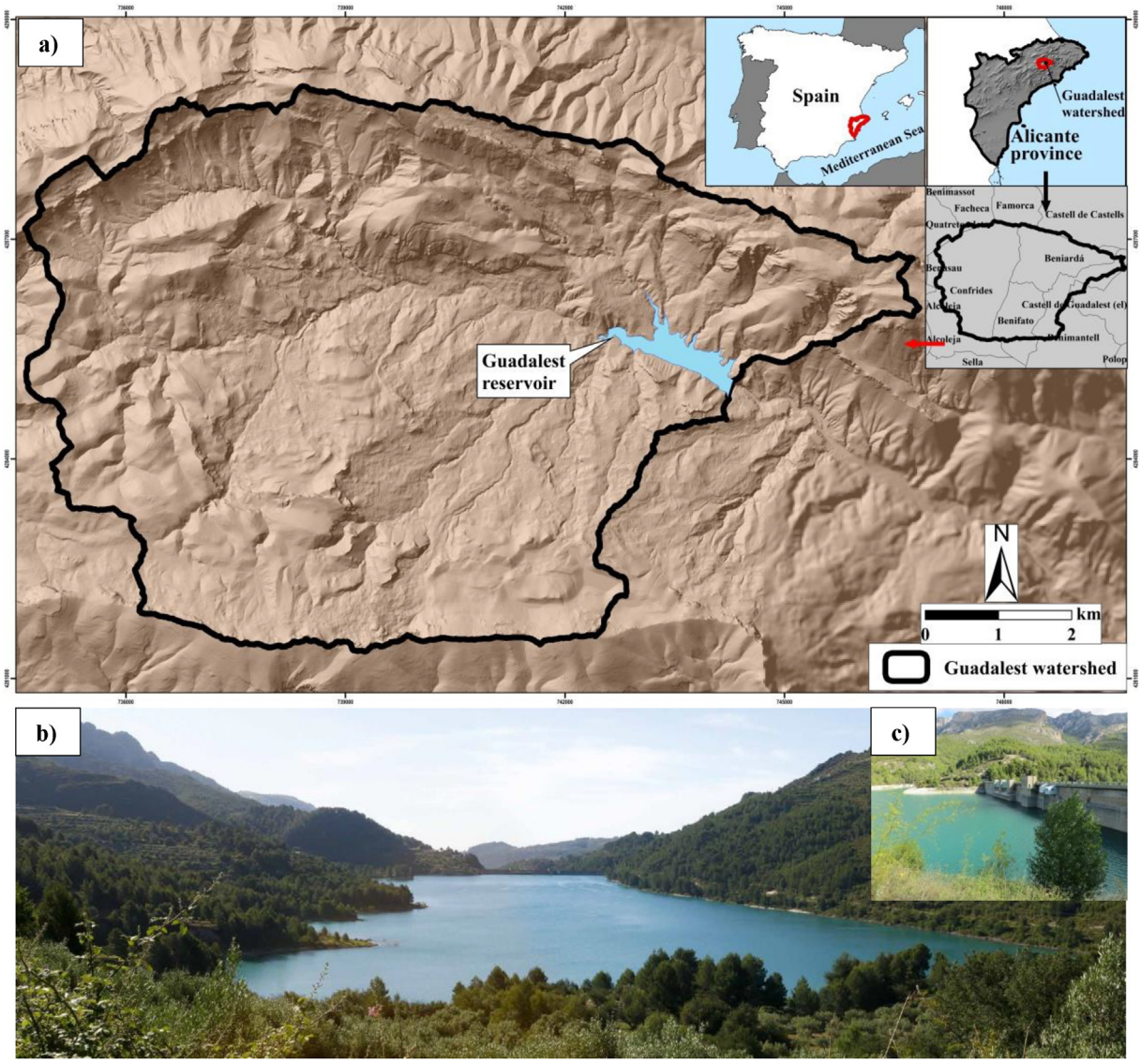

Fig. 1. a) Guadalest hydrographic basin location; b) Panoramic view of the Guadalest reservoir; and c) detail of the reservoir boundary.

Abellan et al., 2017; CHJ, 2013). Precipitation is unevenly distributed along the year, with dry summers and wet autumns (DPA-IGME, 2015; Jodar-Abellan et al., 2018).

The watershed contains outcrops of sedimentary rocks such as limestones, sandstones and conglomerates (53.7%), followed by breccia (18.7%), marls and fine materials (11.6%). The permeability of the main sedimentary rocks is classified as high, medium and low for 17.1, 40.9 and 31.8% of the total surface, respectively (DPA-IGME, 2015; CHJ, 2013; Valdes-Abellan et al., 2018; IGME, 2018). This generates very fast runoff volume production that increases flood risks (Andrade and Szlafsztein, 2018; Ballesteros et al., 2018; Camarasa-Belmonte, 2016; Conesa-García et al., 2017).

Land-uses in the watershed are currently dominated by Mediterranean forests such as coniferous forests, natural grasslands, transitory forests, sclerophyll vegetation, etc. Agriculture occupies scarce areas, being almond and olive groves the most important ones (DPA-IGME, 2015; Valdes-Abellan et al., 2020).

2.2. Methods

2.2.1. Spatial cover information and land-use scenarios

A digital elevation model (DEM) was obtained from the Spanish National Geographic Institute's website (CNIG, 2017) in raster format with a 5-m square cell size. This DEM was prefiltered using ArcGIS 10.6 (ESRI, 2021) to eliminate drains and peaks and, consequently, avoid the generation of a discontinuous drainage system (Tarboton et al., 1991). Next, the drainage network in the watershed was obtained using the mentioned tool. Likewise, a slope map was created and classified into two different classes, 0–3% and >3%, to evaluate the hydrological response and runoff generation (BOE, 2016).

The land-use research and coverage classification was obtained using the Corine Land Cover (CLC) Ministerial Order Project, based on information available in CNIG (2017) in vector format, at a scale of 1:100,000, and with a minimum polygon size of 25 ha. Five different land-use scenarios were considered according to the available information from the CLC. The five scenarios correspond to the years 1990, 2000, 2006, 2012 and 2018. They were named in this investigation as CLC1990, CLC2000, CLC2006, CLC2012, and CLC2018, respectively. According to the CLC project, lad uses identified in the studied area in all scenarios are collected in Table 1. The most extended land-uses are sclerophyll vegetation, natural grasslands and coniferous forests.

Soil types and subsequent permeability were obtained using the digital information developed by the *Instituto Geológico y Minero de España* (IGME) in shapefile format, scale 1:50,000 (IGME, 2018). Each combination of the above factors (i.e., slope classes, soil types and land-uses) was assimilated to

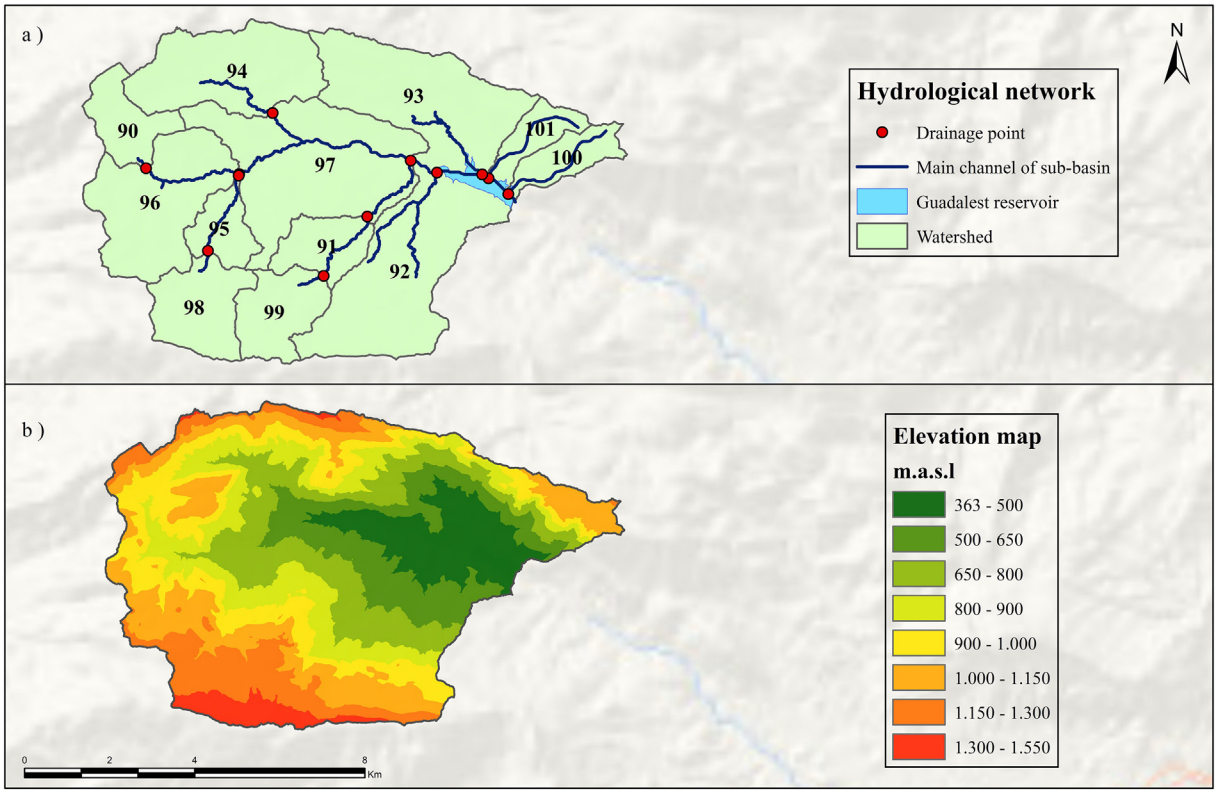

Fig. 2. a) Hydrological network and b) elevation map of the Guadalest watershed.

a runoff threshold according to the Spanish standard 5.2-IC (BOE, 2016), which is an adaptation of the rational method (Cunge, 1969; Slack and Welch, 1980; Tarboton et al., 1991; Candela et al., 2012).

Finally, the total extension of the Guadalest watershed was subdivided into 12 different sub-basins (Fig. 2), trying to consider the drainage network previously obtained from the DEM and seeking the highest homogeneity in terms of runoff generation within each sub-basin, as stated in the investigations published by Mahmood and Jia (2019), Nerantzaki et al. (2020) and Chen et al. (2021). For each sub-basin, characteristics of surface, length and slope of the main channels within the drainage network, as well as concentration-time land-use changes, soil and vegetation types were determined (Table 2). Codes ranging from 90 to 101 were assigned to each sub-basin, as described in Fig. 2.

2.2.2. Climate data and analysis

Climate data was provided by the Spanish National Meteorological Agency (AEMET, 2019). Daily records of precipitation and temperature were obtained from the meteorological stations 8041I-Guadalest and 8040-I located in the urban area of Guadalest and the Guadalest reservoir dam, respectively (CHJ, 2013; DPA-IGME, 2015). The few gaps in the temperature time series were completed with information from the 8025 station, which is close to the watershed (CHJ, 2019; Valdes-Abellan et al., 2020). In particular, there was identified a linear correlation of more than 0.91 between the reference stations and the 8025 stations.

Based on the five temporal scenarios defined according to the land-use coverage, the corresponding average annual precipitation was determined providing values of 375.21, 263.78, 271.20, 352.716, and 249.96 mm for 1984–1989, 1990–1999, 2000–2005, 2006–2011 and 2012–2018 periods, respectively, identifying the lowest value for the final scenario.

The Theil-Sen estimator and the Mann-Kendall (MK) statistical test (Kendall, 1976; Sneyers, 1992; Xueqin and Qiqing, 2005) were performed to assess statistically significant differences (P-value ≤ 0.05) of total annual rainfalls during the studied period (1984–2018). Additionally, a wavelet analysis (Jevrejeva et al., 2003; Grinsted et al., 2004) was carried out to assess the total annual precipitation time series and detect the contribution of the precipitation cycles to the hydrological response and the presence and

Table 1
Land uses codes and nomenclature according to Corine Land Cover.

Codes	Nomenclature
324	Transitory forest/bush
321	Natural grasslands
312	Conifer forest
323	Sclerophyll vegetation
332	Rock outcrops
222	Fruit trees
223	Olive trees
243	Other cultivated fields
512	Water bodies
242	Mixed cultivation fields

Table 2
Main features of the twelve sub-basins in the Guadalest watershed.

Sub-basin	Area (km^2)	Average slope (°)	Length (m)	Tc (h)
90	2.6	3.3	327.7	0.1
91	2.5	6.4	2047.9	0.4
92	9.9	7.5	3119.9	0.5
93	8.9	4.3	2623.5	0.5
94	7.0	4.5	2380.4	0.4
95	2.0	7.2	2134.2	0.4
96	7.2	0.4	2532.2	0.7
97	10.8	3.2	4798.6	0.8
98	3.8	11.4	605.2	0.1
99	3.3	7.7	662.1	0.1
100	2.0	14.6	2910.3	0.4
101	1.8	14.3	2818.8	0.4

magnitude of those cycles. Continuous wavelet transforms (CWT), using Morlet as the mother wavelet, was employed to differentiate the different frequencies contained in the analysed precipitation time series (Pla et al., 2020). The distinction of the different frequencies of the signal allows us to differentiate the contribution of these components (in our case, annual or interannual) to the real recorded signal. In particular, this analysis was performed using the Environmental Wavelet Tool developed by Pla et al. (2020), based on Grinsted et al. (2004) Matlab toolbox.

Finally, potential evapotranspiration was simulated using the Hargreaves method (Hargreaves et al., 1985; Allen et al., 1998), considering the location of the study area and using the temporal series of maximum and minimum temperature.

2.2.3. Hydrological modeling

The hydrological response of the watershed considering different scenarios was simulated through the HEC-HMS (Charley et al., 1995; Koneti et al., 2018). The HEC-HMS model is a physics-based one applied to a wide range of cases, such as climate change impacts on water resources (Abbaspour et al., 2017; Azmat et al., 2018; Liu et al., 2020), land management practices on water, sediment transport, and agricultural chemical yields in calibrated and uncalibrated watersheds (Khoi, 2016; Hu et al., 2021). Recent improvements in this computational time model resolution allow us to conduct the simulation with periods in minutes, placing HEC-HMS as a suitable tool even for flash flood studies (Jeong et al., 2010; Rafiei-Emam et al., 2016; Ferreira et al., 2020). The version used in this research was 4.7 and the simulations were run at a daily scale, which was considered an appropriate computational time step according to the 28-year length period simulated in this study.

The considered hydrological elements were sub-basin, reach, junction, reservoir, diversion, sources and sinks, which were connected in a network to simulate a rainfall-runoff process (Fleming and Brauer, 2018). The computation started from upstream elements to the downstream direction and obtained a classification of different methods to simulate infiltration values (Giménez et al., 1997; Jenicek, 2009; Arnold et al., 2012).

The curve number method (CN), developed by the Soil Conservation Service of the United States (Slack and Welch, 1980; SCS, 1986), was implemented to simulate the rainfall-runoff process. In particular, this method, applicable to small agricultural watersheds after determining the maximum potential soil water retention and precipitation, allows us to estimate the runoff with an acceptable precision (Giménez et al., 1997; Dvoráková et al., 2012; Arnold et al., 2012). The CN can reflect the soil infiltration conditions, the agricultural land management practices, the antecedent condition of rain and the soil cover, which relate to infiltration and runoff rates. The CN value varies from 0 (for completely permeable surfaces) to 100 (for completely impermeable surfaces) (Sraj et al., 2010; D'Asaro et al., 2018). A direct linear relationship was established between the curve number method and runoff threshold contained in the 5.2-IC Spanish regulation (BOE, 2016). Likewise, according to Boongaling et al. (2018) and Elaji and Ji (2020), five different models were established, each one associated with the immediate 6-year period whose final year corresponds to the associated year of land-use according to the above-mentioned scenarios (i.e., CLC2012 corresponds to the years 2007–2012).

The flood propagation along the watercourses was simulated using the linear storage model stated in the Muskingum routing method, which is the most classic example of the use of variable flow-warehousing relations (Cunge, 1969; Khoi, 2016; Overton, 1966). This method is well-established in the hydrological literature and its low data requirement makes it accurate for practical uses (Linsley et al., 1977; D'Asaro et al., 2018). The Muskingum method assumes linear relationships between channel storage, the inflow and the outflow discharge (Overton, 1966), and allows us to depict two main parameters called K and X, which are usually derived by calibration protocols using measured discharge hydrographs (Abbaspour et al., 2017; Azmat et al., 2018; Csáki et al., 2020). In our study, a value of 0.6 was adopted as the response time (K), which represents the transit time of the flow wave in the measured hydrograms according to the characteristics of the basin channels. This procedure agrees with previous investigations published by Cunge (1969) and Overton (1966). For the parameter X, which depends on the storage form and whose value in natural channels is between 0 and 0.5, a value of 0.2 was used according to Sraj et al. (2010), Dvoráková et al. (2012) and Jodar-Abellan et al. (2019).

Likewise, based on available information of the assessed watershed (CHJ, 2013; DPA-IGME, 2015) and related studies areas (Candela et al., 2012; Conesa-García et al., 2017; Đukic and Erić, 2021), baseflow was predicted through the constant monthly baseflow method (Charley et al., 1995; Chen et al., 2021; Mo et al., 2021).

2.2.4. Model calibration and validation

Sensitivity and uncertainly analysis (calibration and validation) were performed at a daily scale using the observed flow data from the 8015 stream gauge station to optimize initial values of hydrologic parameters from the HEC-HMS model. This station is located at the outlet of the Guadalest watershed and contains valuable data from 1967 to 2018 (CEDEX, 2021), which complete hydrogram can be found in CHJ (2013), DPA-IGME (2015), CHJ (2019) and in Fig. 5. According to the five considered land-use scenarios of this study, the observed flow series were divided into periods of four and two years to calibrate and validate the model, respectively. Thus, the HEC-HMS model with land-use cartography of 1990 was calibrated using daily registers from 1988 to 1991 and validated in 1992 and 1993. The rest of the models were classified as follows: for the 2000 scenario, it was calibrated from 1996 to 1999 and validated during 2000 and 2001; the model of 2006 was calibrated from 2002 to 2005 and validated during 2006 and 2007; the 2012 model was calibrated from 2008 to 2011 and validated during 2012 and 2013; and, finally, the 2018 model was calibrated from 2013 to 2016 and validated during 2017 and 2018.

The automatic calibration (in this case deterministic optimization) was focused on the most key parameters of the HEC-HMS model (Fleming and Brauer, 2018) according to the objectives of the present study jointly with findings provided by scientific studies performed in other catchments with similar features (Candela et al., 2012; Azmat et al., 2018; Ferreira et al., 2020; Đukic and Erić, 2021; Chen et al., 2021). Thus, the selected parameter set was composed by: i) the curve number (CN); ii) initial abstraction; iii) lag time recession constant; iv) ratio to peak; v) canopy maximum storage; vi) crop coefficient; vii) soil storage; viii) soil percolation; and, ix) groundwater 1 and 2 percolation rates. Before conducting the calibration and validation, the sensitivity analysis was accomplished to explore the most sensitive parameters in the watershed. According to this analysis, the final parameters set to be optimized were composed by: the curve number (CN), initial abstraction, recession constant, peak ratio, canopy maximum storage, soil storage and soil percolation (Table 3).

Likewise, five statistical contrasts were selected to assess the model performance, considered as the goodness of fit among observed and simulated streamflow: the Nash-Sutcliffe efficiency (NSE), which was chosen in addition as the goal function to be maximized; the mean absolute error (MAE); the root mean square error (RMSE); and the coefficient of determination (R^2). Detailed information about these statistics, together with their optimal values, can be found in Moriasi et al. (2007) and Mahmood and Jia

Table 3
Optimized values of the considered parameters during calibration for each scenario. Note: the values showed in the table are the average for the complete Guadalest watershed calculated from the obtained in each subbasin.

Parameter (units)	Optimized values				
	1990	2000	2006	2012	2018
Curve number (−)	68.4	72.09	72.1	73.71	72.94
Initial abstraction (mm)	61.4	59.72	60.98	53.7	51.8
Recession constant (−)	0.79	0.79	0.79	0.79	0.79
Ratio to peak (−)	0.03	0.03	0.03	0.03	0.03
Canopy max. Storage (mm)	20	15	15	10	5.1
Soil storage (mm)	150	150	150	150	150
Soil percolation (mm/h)	10	10	10	10	10

(2019). Moreover, the new statistical indicator Nash-Sutcliffe efficiency index adapted for arid environments (ANSE) was considered. This index was successfully tested in the Mediterranean arid and semi-arid environments in Valdes-Abellan et al. (2018). Table 4 depicts the model-simulation approach, provided by the considered statistics, during the complete period of calibration and validation.

3. Results and discussion

3.1. Land-use changes and curve number variations

Noticeable land-use changes were observed along the studied period (Table 5). The initial scenarios (CLC1990 and CLC2000) showed mainly areas of sclerophyllous vegetation and agricultural fields, while the most recent scenarios (CLC2006, CLC2012 and CLC2018) showed areas of natural grasslands, coniferous forest, and a reduction in specific cultivated fields such as fruit trees. These changes in land-use respond to the anthropogenic requirement and the demand focused mainly on livestock and fruit plantations, jointly with the high population pressure from close urban areas (Alonso-Sarría et al., 2016; Ballesteros et al., 2018; Camarasa-Belmonte, 2016; García and Cutillas, 2014). This is a topic recently discussed by several scholars who paid attention to the intensification of fruit plantations (tropical and citrus orchards) and high soil and water losses due to bare soils, intense tillage practices and the use of pesticides (Rodrigo-Comino et al., 2020). Similar land-use trends, especially related to agricultural abandonment, are identified in numerous Mediterranean and semi-arid regions globally (Jenicek, 2009; Pérez-González et al., 2017; Hu and Shrestha, 2020; Fortesa et al., 2020). The main causes can be related to aging and depopulation of rural areas (Carbonaro et al., 2018; Pineda, 2001) and less productivity of cultivated lands affected by less fertile and productive soils affected by soil erosion processes (Novara et al., 2016; Rodrigo-Comino, 2018; Romero-Díaz et al., 2017; Lasanta et al., 2021).

Another change was detected in the use of agricultural land (Table 5) during the years 1990, 2000 and 2006 with a decrease of −5.7% for the sub-basin 96 and − 6.2% for the sub-basin 92, respectively. Then, a slight increase in the agricultural lands appeared in 2012 and 2018 (2.5% and 3.1% respectively in the mentioned sub-basins). Recent studies conducted in E and SE Spain (Alonso-Sarría et al., 2016; Cerdà et al., 2021a and Cerdà et al., 2021b; García-Ruiz and Lana-Renault, 2011) suggest that these recent changes in land abandonment of agricultural areas respond to climate-related factors, topographical limitations such as the occurrence of small landslides, as well as numerous socio-economic factors derived from the reduction of subsidies by the European Agricultural Policies, among others. We also hypothesize that reduction in precipitation already identified in the region (Valdes-Abellan et al., 2017) jointly with the controversy about the use of external water resources from other basins (Molina-Giménez and Melgarejo-Moreno, 2015; Sánchez-Galiano et al., 2017; Melgarejo-Moreno et al., 2019; Ricart and Rico, 2019) could be other two additional factors that are reducing the profits of rain-fed agriculture and increasing the risk of irrigated practices promoting the abandonment of the agriculture in this region.

Fig. 3 shows the changes in land-uses from 1990 to 2018, and also shows the differences identified at a sub-basin scale in the optimized curve number levels of sclerophyllous vegetation areas, natural grasslands, agricultural and fruit plantations among others. A close relation between land-use/land cover changes and the curve number trends were identified in the Guadalest watershed, in agreement with previous studies (Jenicek, 2009; D'Asaro et al., 2018; Hu and Shrestha, 2020; Asmar et al., 2021). Thus, the first land-use scenarios (1990, 2000 and 2006) depicted extended areas of olive trees, complex crop patterns with farms and rural exploitations with different sizes, while the last periods (2012 and 2018) showed an important rise of natural areas such as conifer forest, natural grassland, and so one. These land-use changes (agricultural abandonment) generated a relevant increase of the average curve number in the watershed (Fig. 3), from values of 64–65 in the first periods (1990 and 2000) to values up to 75–76 in the last ones (especially in the 2012 scenario). Similar trustworthy results were obtained by Jodar-Abellan et al. (2019) in five basins located in the coastline of the Alicante province, close to the Guadalest watershed. In particular, these authors were able to predict average curve number increases of about 10–15 units for agricultural and forest areas along their land use studied period (from 1990 to 2012). The abandonment of ploughing, linked to common agricultural practices, and the subsequent increase in the soil compaction level may lead to an increase in the soil permeability that would explain the predicted increase in the curve number.

Therefore, as a consequence of the average curve number surged in the Guadalest watershed, less infiltration rates (recharge of aquifers) and several enlargements in the waterproofing factors are expected to occur,

Table 4
Performance of the HEC-HMS model in calibration and validation.

Statistical contrasts			Calibration (240 months)	Validation (120 months)
Acron.	Range	Opt.		
NSE	[−∞, 1]	1	0.51	0.48
MAE	[0, ∞]	0	0.57	0.60
RMSE	[0, ∞]	0	0.77	0.83
R^2	[0,1]	1	0.64	0.67
ANSE	[−∞, 1]	1	0.69	0.72

Table 5
Most representative changes in land use of the twelve sub-basins in the Guadalest watershed.

Sub-basin	USES_CLC	Nomenclature corine	Percentage	
			1990	2018
	323	Sclerophyll vegetation	81.56	0.0
101	321	Natural grasslands	0.0	81.55
	323	Sclerophyll vegetation	95.02	0.0
100	312	Conifer forest	0.0	30.11
	321	Natural grasslands	0.0	31.51
	324	Transitory forest/bush	0.0	36.95
	323	Sclerophyll vegetation	84.38	0.0
99	321	Natural grasslands	0.0	70.76
	333	Scarce vegetation cover	0.0	16.93
	323	Sclerophyll vegetation	100	0.0
98	321	Natural grasslands	0.0	64.30
	312	Conifer forest	0.0	24.72
	323	Sclerophyll vegetation	29.01	0.0
97	242	Cultivated fields	63.58	0.0
	312	Conifer forest	0.0	37.86
	321	Natural grasslands	0.0	14.30
	223	Olive trees	0.0	18.79
	323	Sclerophyll vegetation	64.15	0.0
96	242	Cultivated fields	30.08	0.0
	321	Natural grasslands	0.0	67.09
	323	Sclerophyll vegetation	0.0	19.01
	242	Cultivated fields	49.91	0.0
95	323	Sclerophyll vegetation	50.09	0.0
	321	Natural grasslands	0.0	60.44
	222	Fruit trees	0.0	26.25
	323	Sclerophyll vegetation	90.46	0.0
94	324	Transitory forest/bush	0.0	28.63
	312	Conifer forest	0.0	57.92
	323	Sclerophyll vegetation	68.52	0.0
93	242	Cultivated fields	22.20	0.0
	321	Natural grasslands	0.0	54.82
	312	Conifer forest	0.0	22.44
	242	Cultivated fields	51.64	0.0
92	323	Sclerophyll vegetation	32.30	0.0
	312	Conifer forest	0.0	20.70
	222	Fruit trees	0.0	24.68
	321	Natural grasslands	0.0	19.40
	242	Cultivated fields	84.35	0.0
91	323	Sclerophyll vegetation	15.65	0.0
	222	Fruit trees	0.0	54.19
	323	Sclerophyll vegetation	0.0	20.05
	323	Sclerophyll vegetation	75.84	0.0
90	324	Transitory forest/bush	19.33	0.0
	321	Natural grasslands	0.0	51.15
	312	Conifer forest	0.0	41.03

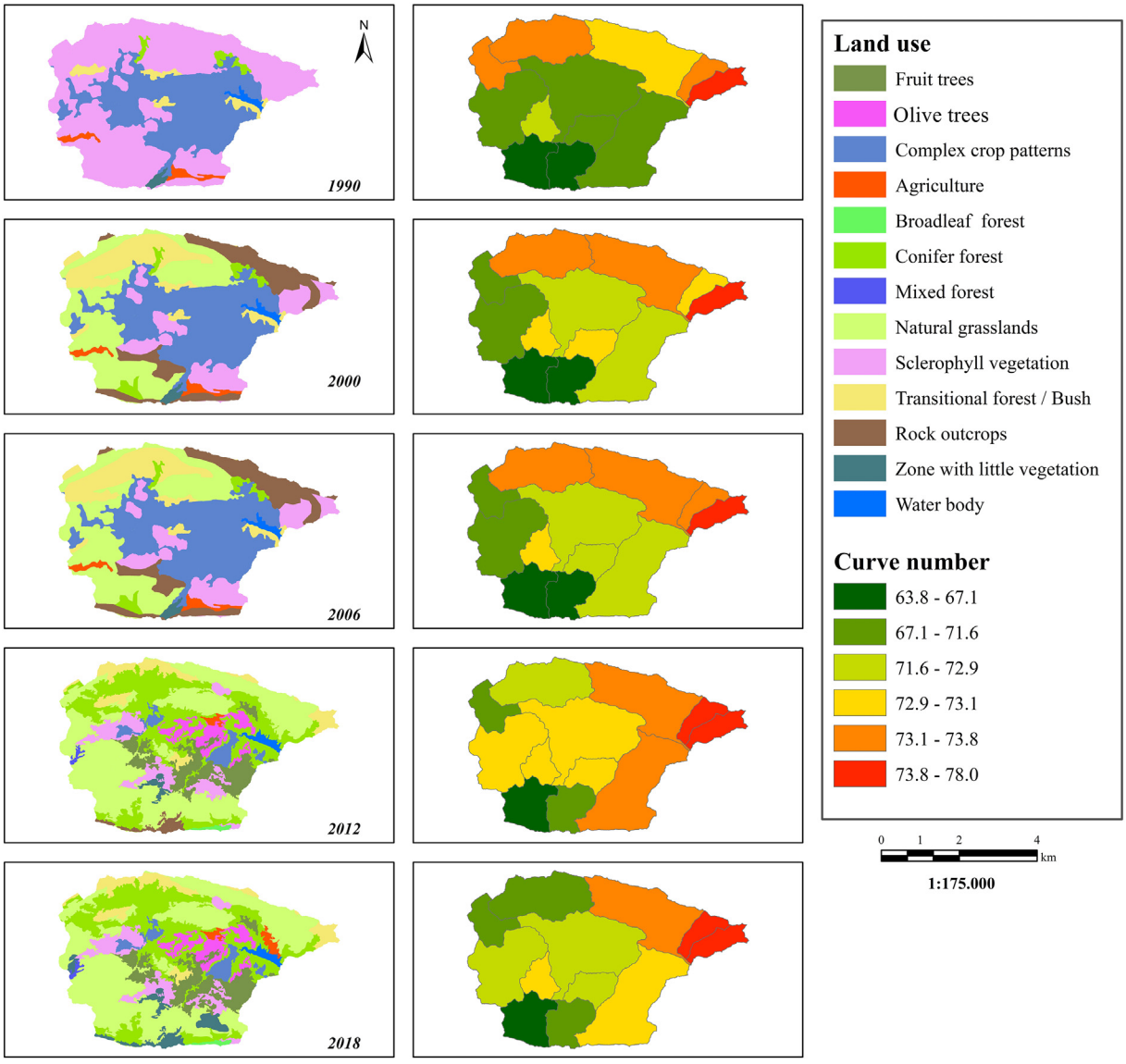

Fig. 3. Land use and curve number variations to the periods: 1990, 2000, 2006, 2012 and 2018 in the Guadalest watershed.

increasing the vulnerability of the terrain (Al Kuisi and El-Naqa, 2013; Andrade and Szlafsztein, 2018; Allam et al., 2020; Nayeb-Yazdi et al., 2021). Thus, it is important to remark the necessity to develop nature-based solutions based on vegetation restoration plans (Kalantari et al., 2018; Keesstra et al., 2018) or to apply sustainable soil management systems for the cultivated areas, for example, reducing the tillage, the use of chemicals and including vegetation cover along with the inter-row areas (Cohen-Shacham et al., 2016; Oral et al., 2020).

3.2. Precipitations trends

The analysis of the total annual precipitation series during the period 1984–2018 showed a cyclical regime and a general decrease attending its linear and 4-year moving average trends mean values of 330 mm/year in 1984–1989 to 270 mm/year in 2014–2018 (Fig. 4a). In particular, the cyclical component of this variable marked approximately four years for each cycle, whether it is rainy or dry, with the driest corresponding to the period 2012–2016. These findings were verified by results obtained from the performed wavelet analysis (Fig. 4b). The application of this analysis showed a significant cycle of four years, which was much more evident in the last decade of the twentieth century. However, in other decades, the presence of this cycle existed but with a lower intensity and with no statistical significance (Fig. 4b). This precipitation pattern can be considered typical from Mediterranean climates characterized by seasonal precipitation changes with an elevated spatial and temporal variability, dry summers and heavy rainfall events (Sraj et al., 2010; Amengual et al., 2015; Conesa-García et al., 2017). The statistical analysis of the total annual precipitations, achieved with the Theil-Sen estimator, depicted a negative trend of −0.66 mm/year from 1984 to 2018 (Fig. 4a). This trend did not show statistically significant differences (P-value < 0.05) according to the performed Mann-Kendall (MK) test, which revealed a P-value of 0.64. However, in the case of analysing total annual precipitation series with a length of 30–35 years, these results are common in Mediterranean areas as the southeast of Spain. For instance, Valdes-Abellan et al. (2017) or Jodar-Abellan et al. (2018) showed P-values among 0.28 and 0.69 in areas close to the Guadalest watershed. Likewise, accomplished statistical analysis exposed the presence of two high outlier values corresponding to 653.1 mm and 568.5 mm in 1989 and 1997 respectively, both observed in the first half of the studied period (Fig. 4a). In the last observed 20 years, there have been high precipitation events but not high values of total annual precipitation, showing the climate change to more arid and at the same time with the high frequency of high-precipitation events.

It is worthy to highlight those comparable results were also obtained by Allam et al. (2020) with a reduction of 44% in the observed precipitation

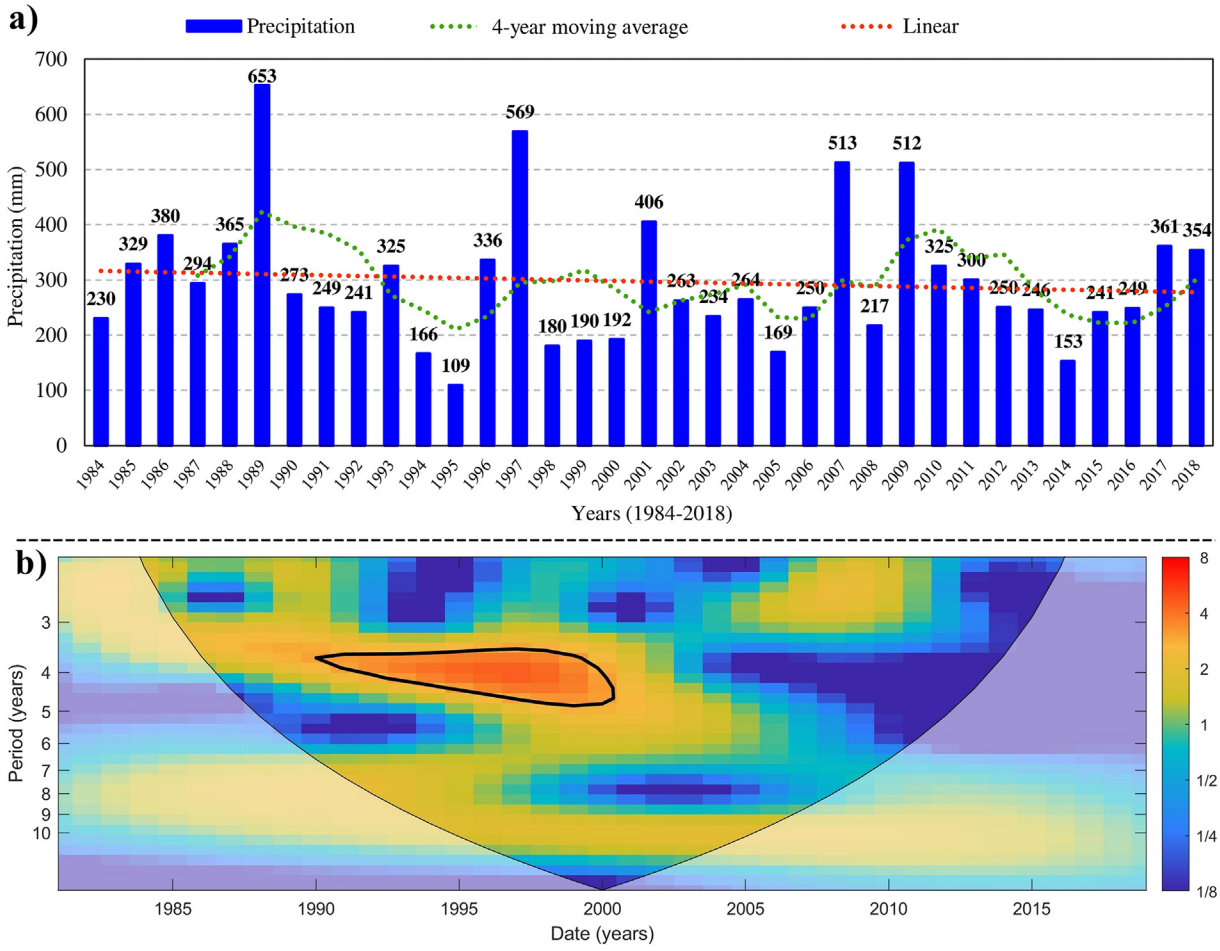

Fig. 4. a) Time series of total annual precipitation in the watershed (period 1984–2018), jointly with the 4-year moving average and linear trend; b) Wavelet analysis of the total annual rainfalls.

rates during the last 50 years (from 1970) in the Mediterranean region. Furthermore, it was also coincident with a higher temperature and reference evapotranspiration increases. Thus, López-Moreno et al. (2009) estimated an average reduction of 8% in the monthly precipitation during the period 1950–2002, in a Mediterranean region that covered Turkey, the Balkans in Italy, Spain, France, the Middle East and some areas of North Africa such as Tunisia. Similar precipitation trends were reported by Caloiero et al. (2018), whose results showed a marked negative rainfall tendency in the eastern Mediterranean with a reduction of more than 20 mm each 10 years and in North Africa (to −16 mm each 10 years), while a relatively large positive trend (more than 20 mm/10 years) was observed in central and northern Europe (Caloiero et al., 2018). Al Kuisi and El-Naqa (2013) assessed average annual precipitation from 1976 to 2005 in the arid Jafr basin (located in Jordan) and observed reductions between 150 and 250 mm. Likewise, Valdes-Abellan et al. (2017) observed in south-eastern Spain a clear change of the precipitation patterns over the last 20 years with annual rainfall reductions between 0% and 15%, increases in the duration of dry periods, and reductions in the number of precipitations events.

Therefore, precipitation trends estimated in the present study are supported by numerous scientific studies accomplished in similar arid and semi-arid Mediterranean regions.

3.3. Streamflow variations

Water discharges were simulated for each sub-basin and the outlet of the Guadalest watershed during the established five scenarios (Fig. 5). Maximum water flows obtained from the model took place in the outlet of the watershed during the following dates: October 1st, 1986 with 137.9 m^3/s; in February 21th, 1992 with 82 m^3/s; on April 17th, 2003 with 60.3 m^3/s; or October 13th, 2007 with 96.6 m^3/s. These maximum flow values are highly correlated with the extreme rainfall episodes observed in the watershed from 1984 to 2018 (Fig. 5). This is corroborated after establishing a correlation up to 0.82 between rainfalls and simulated flows. In the same way, a great correlation among simulated and observed flow rates was obtained, especially reliable in the peak flow events (Fig. 5). Similar trustworthy results of peak flow rates, occurring shortly after an intense rainfall episode associated with convective storms were reported in numerous areas from Southeast of Spain (e.g. Amengual et al., 2015; Camarasa-Belmonte, 2016; Hooke, 2016; Conesa-García et al., 2017; Ballesteros et al., 2018; Jodar-Abellan et al., 2019). A similar idea is observed in several arid and semi-arid regions with similar land-uses, slope classes, soil and topographic features at a global scale (e.g. Rafiei-Emam et al., 2016; Pérez-González et al., 2017; Andrade and Szlafsztein, 2018; Hu and Shrestha, 2020; Asmar et al., 2021). This situation with the more frequent presence of high flow rates events highlights the importance of water flow regulation through a holistic perception of the hydrological cycle, including reforestation of degraded lands, application of socio-economical strategies to avoid agricultural abandonment and the presence of water reservoirs and dams to laminated the maximum flow rates (Boix-Fayos et al., 2020; Gao et al., 2020).

Regarding the analysis of the annual average flows and precipitations during the selected temporal scenarios (Table 6), a close relation between flow and precipitation variations was observed in annual and multiannual terms. Hence, high streamflow rates are generally supported by elevated precipitation values; for instance, during the period 1984–1989, an average rainfall amount of 375 mm/year generated in the watershed an average

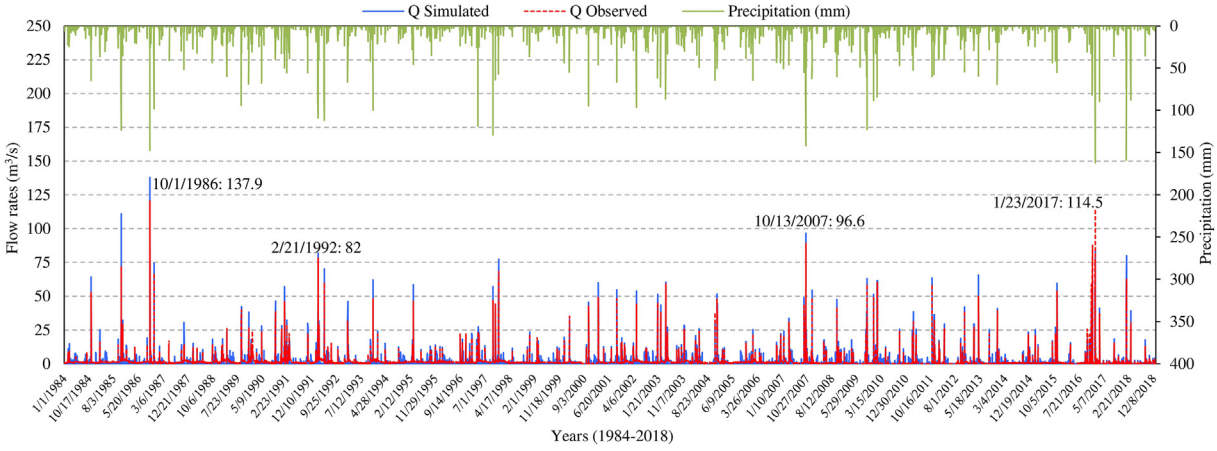

Fig. 5. Rainfall episodes, observed and simulated flows and peak flows during the period 1984–2018, at daily scale, in the watershed outlet. The four highest observed peak flows have been highlighted.

discharge of 15.7 m^3/s (Table 6). Additionally, the above-mentioned curve number variations, as a consequence of the identified land-use changes, depicted an important influence on the flow rates in the watershed. For example, the highest streamflow value (20.3 m^3/s which denotes an increase of 28.8% respect the predicted in 1990) was estimated during the period 2006–2011 (Table 6) as a result of higher precipitation amount (352.7 mm/year) combined with the highest curve number values observed (Fig. 3). This highest curve number value (75.5) depicts an increase of 6.63% concerning previous CN scenarios due to the conversion from land uses with agricultural cover to terrain with rock outcrops, some sparsely natural grassland, etc. It is well-known that higher curve number rates increase surface runoff (streamflow) reducing consequently infiltration and aquifer recharge (Lucas-Borja et al., 2020; Martínez-Retureta et al., 2020). Considering previous issues (drastic land-uses and curve number changes, and especially a clear reduction of the precipitation amount during the period 1984–2018), a moderate decrease in the annual average flows was estimated in the watershed during the mentioned period (Table 6). Similar flow trends were shown by Jodar-Abellan et al. (2018) with an average reduction of 10% in the flow rates and by Valdes-Abellan et al. (2020) with analogous reductions of the surface available water. Both investigations were also performed in arid and semi-arid Mediterranean areas of Southeast Spain. Likewise, in the arid Ten Great Gullies basin (China), Liu et al. (2020) also recognized important reductions of the average annual runoff, among 33% and 41% during their studied period (1964–2011), as a consequence of terrain and human changes.

3.4. Challenges and further research

The hydrological response of a basin obey a group of geomorphological, pedological and climate factors among others when human intervention is added (Bathurst et al., 2004; Chen et al., 2015; Ott and Uhlenbrook, 2004). These factors are not steady along time and potential and unexpected changes may affect whatever aspect of the hydrological cycle such as the runoff generation and its interannual regime from the pedon to the hillslope scale (e.g. Kiani-Harchegani et al., 2019; Minea et al., 2019; Mohammed et al., 2020; Zeraatpisheh et al., 2020). The development of specific vegetation types adapted to the new conditions after the land abandonment can modify the rates of evapotranspiration, aquifer recharge, and even the connectivity processes (Estrany et al., 2019; Hernández et al., 2015), according to the degree of variability in the changing factor. Therefore, we highlight those further studies at the pedon scale focussing on the detection of changes in soil depth, permeability, porosity, organic matter or aggregate stability cannot be obviated (Cammeraat et al., 2010; Novara et al., 2017), since these changes during the coming years could vary our final results using this combined methodology. Also, if precipitation trends change over time, other parameters such as erodibility or water availability for plants and soils will determine new hydrological responses at the hillslope scale (Ayoubi et al., 2018; Hu et al., 2019; Nearing et al., 2004) and should be included in future studies.

In our study, anthropic activities are confirmed as one of the key factors with the highest rates of change at the catchment scale and may present different dynamics both in space and time. This makes that the water cycle of the basin can be modified at the will of the negligence and irresponsibility of anthropic actions or instead to strategic decisions to improve the regulation behaviour of a basin. In the domain of land use and land cover, the vegetation plays a key role through features such as the plant height, plant water demand, root depth, vegetable genotype or the spatial density of the plant coverage.

The present study conducted in the last 34 years (1984–2018) in the Guadalest watershed, has let to identify changes in land use, going from sclerophyllous vegetation in an initial scenario to natural grasslands in the newest scenario. A slight abandonment of agricultural areas was also identified, migrating to natural grasslands and coniferous forests. All those identified changes have led to increases in the curve number values in all sub-basins. We have also identified a reduction trend in the total annual precipitation, which lies underneath the 4-year wet-dry cycles which have also been highlighted. Therefore, it is necessary to observe if these changes will also affect the relationships between soil-water-plants during the coming years and how could be solved. Also, further analysis should be addressed to evaluate the watershed response regarding other land uses, not observed in the past but probable to occur in the future such as an increase in forest, urbanization or wildfires (Salvati, 2014).

4. Conclusions

The effects of the detected changes on the hydrological response of the watershed have been predicted using the HEC-HMS model, implemented at a daily scale, jointly with GIS-based software. These tools have proven to provide useful information for future hydrological stage uses, being this fact especially relevant in karstic environments where research with such methodologies remains limited concerning other domains. In particular, within the HEC-HMS, the SCS Curve Number model and the Muskingum

Table 6
Results of the five scenarios to the average annual flow and to the average annual precipitation at the outlet of the Guadalest watershed.

Stage	Annual average flow (m^3/s)	Annual average precipitation (mm)
1984–1989	15.73	375.21
1990–1999	15.00	263.78
2000–2005	15.61	271.20
2006–2011	20.26	352.72
2012–2018	14.80	249.96

method were suitable for solving the rainfall-runoff conversion and flood propagation equations, respectively. Likewise, calibration and validation of the HEC-HMS model reported satisfactory values of the considered statistical contrasts (NSE, R^2, MAE, RMSE and the new ANSE index). The precipitation in the watershed showed a decreasing trend of rain in the period from 1984 to 2018, together with rainfall cycles of four years which were assessed by own developed wavelet analysis. In particular, these cycles were much more evident (statistically significant) in the last decade of the twentieth century. Thus, we concluded that changes in land-uses (abandonment and intensification of agriculture) were able to modify evaporation and infiltration rates at the watershed scale, which also affect the reduction of runoff in the watershed. These results should assist water managers when establishing strategies to face coming potential environmental hazards such as climate change, loss of soil fertility, transport of contaminants or concentrated runoff peak flows, especially, for vulnerable areas close to rural and urban territories. Moreover, this study allows us to capture the high complexity (orographic and meteorological) of the Mediterranean basins, especially, in water-stressed regions, which are extremely linked to the vulnerability of the population and the perception of socio-environmental risk.

CRediT authorship contribution statement

Teresa Palacios-Cabrera: writing original-draft, software and computations, figures; **Javier Valdes-Abellan**: writing original-draft, conceptualization, writing-review-editing; **Antonio Jodar-Abellan**: writing original-draft, literature review, writing-review-editing, figures, software improvement; **Jesús Rodrigo-Comino**: writing original-draft, conceptualization, figures, writing-review editing.

Declaration of competing interest

The authors declare that they have no known competing financial interests or personal relationships that could have appeared to influence the work reported in this paper.

Acknowledgements

This research was funded partially by the Central University of Ecuador and by the projects RESERVOIR (PRIMA programme supported by the European Union under grant agreement no. 1924) and BBVA2021-Leonardo2 along with local companies (projects *Comunidad Regantes* 2-20I and *Comunidad Regantes* 1-20T). Antonio Jodar-Abellan acknowledges financial support received from the project BBVA2021-Leonardo2. In the same way, this work has been conducted within the Cátedra del Agua of the University of Alicante (catedradelaguaua.org). Moreover, authors acknowledge the reviewers of the manuscript whose comments contributed greatly to improve this paper.

References

Abbaspour, K.C., Vaghefi, S.A., Srinivasan, R., 2017. A guideline for successful calibration and uncertainty analysis for soil and water assessment: a review of papers from the 2016 international SWAT conference. Water 10 (1).

Aburas, M.M., Ahamad, M.S.S., Omar, N.Q., 2019. Spatio-temporal simulation and prediction of land-use change using conventional and machine learning models: a review. Environ. Monit. Assess. 191. https://doi.org/10.1007/s10661-019-7330-6.

AEMET, 2019. Registers of the Spanish National Meteorologial Agency.

Al Kuisi, M., El-Naqa, A., 2013. GIS based Spatial Groundwater Recharge estimation in the Jafr basin, Jordan-Application of WetSpass models for arid regions. Revista Mexicana de Ciencias Geológicas 30 (1), 96–109.

Allam, A., Moussa, R., Najem, W., Bocquillon, C., 2020. Hydrological cycle, Mediterranean basins hydrology. Water Resources in the Mediterranean Region. Elsevier Inc. ISBN 9780128180860.

Allen, R.G., Pereira, L.S., Raes, D., Martin, S., 1998. Crop evapotranspiration - guidelines for computing crop water requirements - FAO irrigation and drainage paper 56. Food and Agriculture Organization of the United Nations, Rome.

Alonso-Sarría, F., Martínez-Hernández, C., Romero-Díaz, A., Cánovas-García, F., Gomariz-Castillo, F., 2016. Main environmental features leading to recent land abandonment in Murcia region (Southeast Spain). Land Degrad. Dev. 27 (3), 654–670.

Amengual, A., Homar, V., Jaume, O., 2015. Potential of a probabilistic hydrometeorological forecasting approach for the 28 september 2012 extreme flash flood in Murcia, Spain. Atmos. Res. 166, 10–23.

Andrade, M.M.N., Szlafsztein, C.F., 2018. Vulnerability assessment including tangible and intangible components in the index composition: an Amazon case study of flooding and flash flooding. Sci. Total Environ. 630, 903–912.

Arnold, J.G., Kiniry, J.R., Srinivasan, R., Williams, J.R., Haney, E.B., Neitsch, S.L., 2012. nput/Output Documentation. Version 2012. TR-439. 650 ppTexas Water Resources Institute. http://swat.tamu.edu/documentation/2012-io/.

Arnold, J.G., Srinivasan, R., Muttiah, R.S., Williams, J.R., 1998. Large area hydrologic modeling and assessment part I: model development. J. Am. Water Resour. Assoc. 34 (1), 73–89.

Asmar, N.F., Sim, J.O., Ghodieh, A., Fauzi, R., 2021. Effect of land use/Land cover changes on estimated potential runoff in the Nablus mountains watersheds of Palestine: a case study. J. Indian Soc. Remote Sens. https://doi.org/10.1007/s12524-020-01278-2.

Assefa, F., Elias, E., Soromessa, T., Ayele, G.T., 2020. Effect of changes in land-use management practices on soil physicochemical properties in Kabe Watershed, Ethiopia. Air Soil Water Res. 13, 1178622120939587. https://doi.org/10.1177/1178622120939587.

Ayoubi, S., Mokhtari, J., Mosaddeghi, M.R., Zeraatpisheh, M., 2018. Erodibility of calcareous soils as influenced by land use and intrinsic soil properties in a semiarid region of Central Iran. Environ. Monit. Assess. 190. https://doi.org/10.1007/s10661-018-6557-y.

Azmat, M., Qamar, M.U., Huggel, C., Hussain, E., 2018. Future climate and cryosphere impacts on the hydrology of a scarcely gauged catchment on the jhelum river basin, northern Pakistan. Sci. Total Environ. 639, 961–976. https://doi.org/10.1016/j.scitotenv.2018.05.206.

Ballesteros, C., Jiménez, J.A., Viavattene, C., 2018. A multi-component flood risk assessment in the maresme coast (NW Mediterranean). Nat. Hazards 90 (1), 265–292.

Bathurst, J.C., Ewen, J., Parkin, G., O'Connell, P.E., Cooper, J.D., 2004. Validation of catchment models for predicting land-use and climate change impacts. 3. Blind validation for internal and outlet responses. J. Hydrol. 287, 74–94.

BOE, 2016. Proyecto de Orden Ministerial por la que se aprueba la Norma 5.2-IC Drenaje Superficial de la Instrucción de Carreteras. Boletín Oficial del Estado (BOE).

Boix-Fayos, C., Boerboom, L.G.J., Janssen, R., Martínez-Mena, M., Almagro, M., Pérez-Cutillas, P., Eekhout, J.P.C., Castillo, V., De Vente, J., 2020. Mountain ecosystem services affected by land use changes and hydrological control works in Mediterranean catchments. Ecosyst. Serv. 44, 101136. https://doi.org/10.1016/j.ecoser.2020.101136.

Boongaling, C.G.K., Faustino-Eslava, D.V., Lansigan, F.P., 2018. Modeling land use change impacts on hydrology and the use of landscape metrics as tools for watershed management: the case of an ungauged catchment in the Philippines. Land Use Policy 72, 116–128.

Brunner, G.W., Bonner, V.R., 1994. HEC River Analysis System (HEC-RAS). ASCE National Conference on Hydraulic Engineering, Buffalo, New York. 16 ppUS Army Corps of Engineers-Hydrologic Engineering Center (TP-147) http://www.hec.usace.army.mil/publications/.

Buonocore, C., Gomiz-Pascual, J.J., Pérez-Cayeiro, M.L., Mañanes-Salinas, R., Mejías, M.B., 2021. Modelling the impacts of climate and land use changes on water quality in the Guadiana basin and the adjacent coastal area. Sci. Total Environ. 776, 146034.

Caloiero, T., Caloiero, P., Frustaci, F., 2018. Long-term precipitation trend analysis in Europe and in the Mediterranean basin. Water Environ. J. 32, 433–445.

Camarasa-Belmonte, A.M., 2016. Flash floods in Mediterranean ephemeral streams in Valencia region (Spain). J. Hydrol. 541, 99–115.

Cammeraat, E.L., Cerdà, A., Imeson, A.C., 2010. Ecohydrological adaptation of soils following land abandonment in a semi-arid environment. Ecohydrology 3, 421–430.

Candela, L., Tamoh, K., Olivares, G., Gomez, M., 2012. Modelling impacts of climate change on water resources in ungauged and data-scarce watersheds. Application to the Siurana catchment (NE Spain). Sci. Total Environ. 440, 253–260. https://doi.org/10.1016/j.scitotenv.2012.06.062.

Carbonaro, G., Leanza, E., McCann, P., Medda, F., 2018. Demographic decline, population aging, and modern financial approaches to urban policy. Int. Reg. Sci. Rev. 41, 210–232. https://doi.org/10.1177/0160017616675916.

CEDEX, 2021. Centro de Estudios y Experimentación de Obras Públicas. Embalse 8015-Guadalest. https://ceh.cedex.es/anuarioaforos/afo/embalse-datos_descarga.asp?ref_ceh=8015. (Accessed 1 August 2021).

Cerdà, A., Novara, A., Dlapa, P., López-Vicente, M., Úbeda, X., Popovic, Z., Mekonnen, M., Terol, E., Janizadeh, S., Mbarki, S., Saldanha-Vogelmann, E., Hazrati, S., Sannigrahi, S., Parhizkar, M., Giménez-Morera, A., 2021. Rainfall and water yield in Macizo del Caroig, Eastern Iberian Peninsula. Event runoff at plot scale during a rare flash flood at the Barranco de Benacancil. Cuad. Investig. Geográfica https://doi.org/10.18172/cig.4833.

Cerdà, A., Franch-Pardo, I., Novara, A., Sannigrahi, S., Rodrigo-Comino, J., 2021b. Examining the effectiveness of catch crops as a nature-based solution to mitigate surface soil and water losses as an environmental regional concern. Earth Syst. Environ. https://doi.org/10.1007/s41748-021-00284-9.

Charley, W., Pabst, A., Peters, J., 1995. The Hydrologic Modeling System (HEC-HMS): Design and Development Issues. ASCE 2nd Congress on Computing in Civil Engineering, Atlanta, Georgia. 16 ppUS Army Corps of Engineers-Hydrologic Engineering Center (TP-149) http://www.hec.usace.army.mil/publications/.

Chen, G., Hua, W., Fang, X., Wang, C., Li, X., 2021. Distributed-framework basin modeling system: II. Hydrologic modeling system. Water 13 (5), 744. https://doi.org/10.3390/w13050744.

Chen, M., Willgoose, G.R., Saco, P.M., 2015. Evaluation of the hydrology of the IBIS land surface model in a semi-arid catchment. Hydrol. Process. 29, 653–670. https://doi.org/10.1002/hyp.10156.

CHJ, 2013. Plan Director de Defensa contra las avenidas. Comarca de la Marina Baja. Alicante. . https://www.chj.es/Descargas/ProyectosDT/MARINA%20BAJA%20DEFINITIVA/PLAN%20DIRECTOR%20MARINA%20BAIXA/DOCUMENTO%201.%20MEMORIA/MEMORIA.pdf.
CHJ, 2019. Confederación Hidrográfica del Júcar. http://aps.chj.es/down/html/descargas.html. (Accessed 5 September 2019).
CNIG, 2017. Centro Nacional de Información Geográfica. Madrid.
Cohen-Shacham, E., Janzen, C., Maginnis, S., Walters, G., 2016. Nature-based solutions to address global societal challenges.
Conesa-García, C., García-Lorenzo, R., Pérez-Cutillas, P., 2017. Flood hazards at ford stream crossings on ephemeral channels (south-east coast of Spain). Hydrol. Process. 31 (3), 731–749.
Csáki, P., Gyimóthy, K., Kaliez, P., Szolgay, J., Zagyvai-Kiss, K., 2020. Multi-model climatic water balance prediction in the Zala River basin (Hungary) based on a modified budyko framework. J. Hydrol. Hydromech. 68, 200–210.
Cunge, J.A., 1969. On the subject of a flood propagation computation method (Muskingum method). J. Hydraul. Res. 7 (2), 205–230.
D´Asaro, F., Grillone, G., Hawkins, R., ASCE, F., 2018. Curve numbers seasonal variation in Mid-Mediterranean Area. 144 (9), 04018021.
DPA-IGME, 2015. Atlas hidrogeológico de la provincia de Alicante: Excelentísima Diputación Provincial de Alicante (DPA)-Ciclo Hídrico. Instituto Geológico y Minero de España (IGME).
Đukic, V., Erić, R., 2021. SHETRAN and HEC HMS model evaluation for runoff and soil moisture simulation in the Jičinka River catchment (Czech Republic). Water. 13 (6), 872.
Dvoráková, S., Kovár, P., Zeman, J., 2012. Implementation of conceptual linear storage model of runoff with diurnal fluctuation in rainless periods. J. Hydrol. Hydromech. 60 (4), 217–226.
Elaji, A., Ji, W., 2020. Urban runoff simulation: how do land use/cover change patterning and geospatial data quality impact model outcome? Water 12, 2715.
ESRI, 2021. ArcGIS software. Environmental Systems Research Institute (ESRI). Available in: https://www.esri.com/en-us/home.
Estrany, J., Ruiz, M., Calsamiglia, A., Carriquí, M., García-Comendador, J., Nadal, M., Fortesa, J., López-Tarazón, J.A., Medrano, H., Gago, J., 2019. Sediment connectivity linked to vegetation using UAVs: high-resolution imagery for ecosystem management. Sci. Total Environ. 671, 1192–1205. https://doi.org/10.1016/j.scitotenv.2019.03.399.
Ferreira, C.S.S., Mourato, S., Kasanin-Grubin, M., Ferreira, A.J.D., Destouni, G., Kalantari, Z., 2020. Effectiveness of nature-based solutions in mitigating flood Hazard in a Mediterranean peri-urban catchment. Water. 12 (10), 2893. https://doi.org/10.3390/w12102893.
Fleming, M., Brauer, T., 2018. Hydrologic Modeling System HEC-HMS. Guide. Version 4.3. 61 pp. Available at:Hydrologic Engineering Center-US. https://www.hec.usace.army.mil/software/hec-hms/.
Fortesa, J., Latron, J., García-Comendador, J., Tomàs-Burguera, M., Company, J., Calsamiglia, A., Estrany, J., 2020. Multiple temporal scales assessment in the hydrological response of small Mediterranean-climate catchments. Water 12, 299.
Gao, Y., Chen, J., Luo, H., Wang, H., 2020. Prediction of hydrological responses to land use change. Sci. Total Environ. 708, 134998.
García, C.C., Cutillas, P.P., 2014. Alteraciones geomorfológicas recientes en los sistemas fluviales mediterráneos de la península ibérica. Síntomas y problemas de incisión en los cauces. Revista de Geografia Norte Grande 59, 25–44.
García-Ruiz, J.M., Lana-Renault, N., 2011. Hydrological and erosive consequences of farmland abandonment in Europe, with special reference to the Mediterranean region - a review. Agric. Ecosyst. Environ. 140 (3–4), 317–338.
Gassman, P.W., Reyes, M.R., Green, C.H., Arnold, J.G., 2007. The soil and water assessment tool: historical development, applications and future research directions. Trans. Am. Soc. Agric. Eng. 50 (4), 1211–1250.
Giménez, D., Perfect, E., Rawls, W.J., Pachepsky, Y., 1997. Fractal models for predicting soil hydraulic properties: a review. Eng. Geol. 48 (3–4), 161–183.
Grinsted, A., Moore, J.C., Jevrejeva, S., 2004. Application of the cross wavelet transform and wavelet coherence to geophysical time series. Nonlinear Process. Geophys. 11, 561–566. https://doi.org/10.5194/npg-11-561-2004.
Hargreaves, G.L., Hargreaves, G.H., Riley, J.P., 1985. Agricultural benefits for Senegal River basin. J. Irrig. Drain. Eng. 111 (2), 113–124.
Hernández, A., Miranda, M., Arellano, E.C., Saura, S., Ovalle, C., 2015. Landscape dynamics and their effect on the functional connectivity of a Mediterranean landscape in Chile. Ecol. Indic. 48, 198–206. https://doi.org/10.1016/j.ecolind.2014.08.010.
Hooke, J.M., 2016. Geomorphological impacts of an extreme flood in SE Spain. Geomorphology 263, 19–38.
Hu, C., Ran, G., Li, G., Yu, Y., Wu, Q., Yan, D., Jian, S., 2021. The effects of rainfall characteristics and land use and cover change on runoff in the Yellow River basin, China. J. Hydrol. Hydromech. 69, 29–40.
Hu, S., Li, L., Chen, L., Cheng, L., Yuan, L., Huang, X., Zhang, T., 2019. Estimation of soil erosion in the Chaohu Lake Basin through modified soil erodibility combined with gravel content in the RUSLE model. Water 11, 1806. https://doi.org/10.3390/w11091806.
Hu, S., Shrestha, P., 2020. Examine the impact of land use and land cover changes on peak discharges of a watershed in the midwestern United States using the HEC-HMS model. Pap. Appl. Geogr. 6 (2), 101–118.
IGME, 2018. Permeability Map of Spain in shapefile format. Scale 1/200.000. Instituto Geológico y Minero de España.
Jenicek, M., 2009. Runoff changes in areas differing in land-use in the blanice river basin-application of the deterministic model. J. Hydrol. Hydromech. 57 (3), 154–161.
Jeong, J., Kannan, N., Arnold, J., Glick, R., Gosselink, L., Srinivasan, R., 2010. Development and integration of sub-hourly rainfall-runoff modeling capability within a watershed model. Water Resour. Manag. 24 (15), 4505–4527.
Jevrejeva, S., Moore, J.C., Grinsted, A., 2003. Influence of the Arctic oscillation and El Niño-southern oscillation (ENSO) on ice conditions in the Baltic Sea: the wavelet approach. J. Geophys. Res. 108 (D21), 4677. https://doi.org/10.1029/2003JD003417.
Jodar-Abellan, A., Ruiz, M., Melgarejo, J., 2018. Climate change impact assessment on a hydrologic basin under natural regime (SE, Spain) using a SWAT model. Revista Mexicana de Ciencias Geológicas 35, 240–253.
Jodar-Abellan, A., Valdes-Abellan, J., Pla, C., Gomariz-Castillo, F., 2019. Impact of land use changes on flash flood prediction using a sub-daily SWAT model in five Mediterranean ungauged watersheds (SE Spain). Sci. Total Environ. 657, 1578–1591.
Kalantari, Z., Ferreira, C.S.S., Keesstra, S., Destouni, G., 2018. Nature-based solutions for flood-drought risk mitigation in vulnerable urbanizing parts of East-Africa. Curr. Opin. Environ. Sci. Health 5, 73–78. https://doi.org/10.1016/j.coesh.2018.06.003.
Keesstra, S., Nunes, J., Novara, A., Finger, D., Avelar, D., Kalantari, Z., Cerdà, A., 2018. The superior effect of nature based solutions in land management for enhancing ecosystem services. Sci. Total Environ. 610–611, 997–1009. https://doi.org/10.1016/j.scitotenv.2017.08.077.
Kendall, S., 1976. Time Series. 2nd edition. Oxford University Press, New York 198 pp.
Khoi, D.N., 2016. Comparison of the HEC-HMS and SWAT hydrological models in simulating the stream flow. J. Sci. Technol. 53 (5), 189–195.
Kiani-Harchegani, M., Sadeghi, S.H., Singh, V.P., Asadi, H., Abedi, M., 2019. Effect of rainfall intensity and slope on sediment particle size distribution during erosion using partial eta squared. Catena https://doi.org/10.1016/j.catena.2019.01.006.
Koneti, S., Sunkara, S.L., Roy, P.S., 2018. Hydrological modeling with respect to impact of land-use and land-cover change on the runoff dynamics in Godavari river basin using the HEC-HMS model. ISPRS Int. J. Geo Inf. 7 (6).
Lasanta, T., Nadal-Romero, E., Khorchani, M., Romero-Díaz, A., 2021. A review of abandoned lands in Spain: from local landscapes to global management strategies. Geogr. Res. Lett. 47 (2), 477–521.. http://doi.org/10.18172/cig.4755.
Linsley, R., Kohler, M., Paulus, J., 1977. Hidrología para Ingenieros. McGraw-Hill, p. 398.
Liu, T., Huang, H., Shao, M., Cheng, J., Li, X., Lu, J., 2020. Integrated assessment of climate and human contributions to variations in streamflow in the Ten Great Gullies Basin of the Upper Yellow River, China. J. Hydrol. Hydromech. 68, 249–259.
López-Moreno, J.I., Vicente-Serrano, S.M., Gimeno, L., Nieto, R., 2009. Stability of the seasonal distribution of precipitation in the Mediterranean region: observations since 1950 and projections for the 21st century. Geophys. Res. Lett. 36.
Lucas-Borja, M.E., Gianmarco-Carrà, B., Nunes, J.P., Bernard-Jannin, L., Zema, D.A., Zimbone, S.M., 2020. Impacts of land-use and climate changes on surface runoff in a tropical forest watershed (Brazil). Hydrol. Sci. J. 65 (11), 1956–1973. https://doi.org/10.1080/02626667.2020.1787417.
Mahmood, R., Jia, S., 2019. Assessment of hydro-climatic trends and causes of dramatically declining stream flow to Lake Chad, Africa, using a hydrological approach. Sci. Total Environ. 675, 122–140. https://doi.org/10.1016/j.scitotenv.2019.04.219.
Martínez-Retureta, R., Aguayo, M., Stehr, A., Sauvage, S., Echeverría, C., Sánchez-Pérez, J.M., 2020. Effect of land Use/Cover change on the hydrological response of a southern Center Basin of Chile. Water. 12, 302. https://doi.org/10.3390/w12010302.
Mcdonald, M.G., Harbaugh, A.W., 1984. A modular three-dimensional finite-difference ground-water flow model. 539 ppU.S. Geological Survey . https://pubs.er.usgs.gov/publication/ofr83875.
Melgarejo-Moreno, J., López-Ortiz, M.I., Fernández-Aracil, P., 2019. Water distribution management in south-East Spain: a guaranteed system in a context of scarce resources. Sci. Total Environ. 648, 1384–1393.
Minea, G., Ioana-Toroimac, G., Moro, G., 2019. The dominant runoff processes on grassland versus bare soil hillslopes in a temperate environment - an experimental study. J. Hydrol. Hydromech. 67, 8. https://doi.org/10.2478/johh-2019-0018.
Mo, C., Wang, Y., Ruin, Y., Qin, J., Zhang, M., Sun, G., Jin, J., 2021. The effect of karst system occurrence on flood peaks in small watersheds, Southwest China. Hydrol. Res. 52 (1), 305–322.. https://doi:10.2166/nh.2020.061.
Mohammed, S., Alsafadi, K., Talukdar, S., Kiwan, S., Hennawi, S., Alshihabi, O., Sharaf, M., Harsanyie, E., 2020. Estimation of soil erosion risk in southern part of Syria by using RUSLE integrating geo informatics approach. Remote Sens. Appl. Soc. Environ. 20, 100375. https://doi.org/10.1016/j.rsase.2020.100375.
Molina-Giménez, A., Melgarejo-Moreno, J., 2015. Water policy in Spain: seeking a balance between transfers, desalination and wastewater reuse. Int. J. Water Resour. Dev. 32, 781–798.
Molina-Sanchis, I., Lázaro, R., Arnau-Rosalén, E., Calvo-Cases, A., 2016. Rainfall timing and runoff: the influence of the criterion for rain event separation. J. Hydrol. Hydromech. 64 (3), 226–236.
Moriasi, D.N., Arnold, J.G., Van Liew, M.W., Bingner, R.L., Harmel, R.D., Veith, T.L., 2007. Model evaluation guidelines for systematic quantification of accuracy in watershed simulations. Trans. ASABE 50, 885–900. https://doi.org/10.13031/2013.23153.
Nayeb-Yazdi, M., Sample, D.J., Scott, D., Wang, X., Ketabchy, M., 2021. The effects of land use characteristics on urban stormwater quality and watershed pollutant loads. Sci. Total Environ. 773, 145358.
Nearing, M.A., Pruski, F.F., O'Neal, M.R., 2004. Expected climate change impacts on soil erosion rates: a review. J. Soil Water Conserv. 59, 43–50.
Nerantzaki, S.D., Hristopulos, D.T., Nikolaidis, N.P., 2020. Estimation of the uncertainty of hydrologic predictions in a karstic Mediterranean watershed. Sci. Total Environ. 717, 137131.
Nguyen, V.T., Dietrich, J., Uniyal, B., 2020. Modeling interbasin groundwater flow in karst areas: model development, application, and calibration strategy. Environ. Model. Softw. 124, 104606.
Novara, A., Gristina, L., Sala, G., Galati, A., Crescimanno, M., Cerda, A., Badalamenti, E., La Mantia, T., 2017. Agricultural land abandonment in Mediterranean environment provides ecosystem services via soil carbon sequestration. Sci. Total Environ. 576, 420–429. https://doi.org/10.1016/j.scitotenv.2016.10.123.
Novara, A., Keesstra, S., Cerdà, A., Pereira, P., Gristina, L., 2016. Understanding the role of soil erosion on CO2-c loss using 13c isotopic signatures in abandoned Mediterranean agricultural land. Sci. Total Environ. 550, 330–336. https://doi.org/10.1016/j.scitotenv.2016.01.095.

Ollivier, C., Mazzilli, N., Olioso, A., Chalikakis, K., Carrière, S.D., Danquigny, C., Emblanch, C., 2020. Karst recharge-discharge semi distributed model to assess spatial variability of flows. Sci. Total Environ. 703, 134368. https://doi.org/10.1016/j.scitotenv.2019.134368.

Oral, H.V., Carvalho, P., Gajewska, M., Ursino, N., Masi, F., van Hullebusch, E.D., Kazak, J.K., Exposito, A., Cipolletta, G., Andersen, T.R., Finger, D.C., Simperler, L., Regelsberger, M., Rous, V., Radinja, M., Buttiglieri, G., Krzeminski, P., Rizzo, A., Dehghanian, K., Nikolova, M., Zimmermann, M., 2020. A review of nature-based solutions for urban water management in european circular cities: a critical assessment based on case studies and literature. Blue-Green Syst. 2, 112–136. https://doi.org/10.2166/bgs.2020.932.

Ott, B., Uhlenbrook, S., 2004. Quantifying the impact of lans-use changes at the event and seasonal time scale using a process-oriented catchment model. Hydrol. Earth Sytsem Sci. 8, 62–78.

Overton, D.E., 1966. Muskingum flood routing of upland streamflow. J. Hydrol. 4, 185–200.

Pardo, M.Á., Fernández, H., Jodar-Abellan, A., 2020. Converting a water pressurized network in a small town into a solar power water system. Energies 13 (15), 4013.

Peña-Angulo, D., Estrany, J., García-Comendador, J., Fortesa, J., Tomàs-Burguera, M., Company, J., Alorda, B., Nadal-Romero, E., 2021. Influence of weather types on the hydrosedimentary response in three small catchments on the Island of Mallorca, Spain. Environ. Res. 192, 110324. https://doi.org/10.1016/j.envres.2020.110324.

Pérez-González, M.L., Capra-Pedol, L., Dávila-Hernández, N., Borselli, L., Solís-Valdez, S., Ortiz-Rodríguez, A.J., 2017. Spatio-temporal land-use changes in the Colima-Villa de Álvarez metropolitan area, and their relationship to floodings. Revista Mexicana de Ciencias Geológicas 34 (2), 78–90.

Petchprayoon, P., Blanken, P.D., Ekkawatpanit, C., Hussein, K., 2010. Hydrological impacts of land use/land cover change in a large river basin in Central-Northern Thailand. Int. J. Climatol. 30 (13), 1917–1930.

Pineda, F.D., 2001. Intensification, rural abandonment and nature conservation in Spain. Examples of european Agri-environment schemes and livestock systems and their influence on spanish cultural landscapes. Alterra Rapp 309, 23–38.

Pla, C., Fernandez-Cortes, A., Cuezva, S., Galiana-Merino, J.J., Cañaveras, J.C., Sanchez-Moral, S., Benavente, D., 2020. Insights on climate-driven fluctuations of cave 222Rn and CO2 concentrations using statistical and wavelet analyses. Geofluids https://doi.org/10.1155/2020/8858295 1–17 pages.

Rafiei-Emam, A., Mishra, B.K., Kumar, P., Masago, Y., Fukushi, K., 2016. Impact assessment of climate and land-use changes on flooding behavior in the Upper Ciliwung River, Jakarta, Indonesia. Water 8, 559.

Ricart, S., Rico, A.M., 2019. Assessing technical and social driving factors of water reuse in agriculture: a review on risks, regulation and the yuck factor. Agric. Water Manag. 217, 426–439. https://doi.org/10.1016/j.agwat.2019.03.017.

Robineau, T., Tognelli, A., Goblet, P., Renard, F., Schaper, L., 2018. A double medium approach to simulate groundwater level variations in a fissured karst aquifer. J. Hydrol. 565, 861–875. https://doi.org/10.1016/j.jhydrol.2018.09.002.

Rodrigo-Comino, J., Ponsoda-Carreres, M., Salesa, D., Terol, E., Gyasi-Agyei, Y., Cerdà, A., 2020. Soil erosion processes in subtropical plantations (Diospyros kaki) managed under flood irrigation in eastern Spain. Singap. J. Trop. Geogr. 41, 120–135. https://doi.org/10.1111/sjtg.12307.

Rodrigo-Comino, J., 2018. Five decades of soil erosion research in "terroir"The State-of-the-Art. Earth Sci. Rev. 179, 436–447. https://doi.org/10.1016/j.earscirev.2018.02.014.

Romero-Díaz, A., Ruiz-Sinoga, J.D., Robledano-Aymerich, F., Brevik, E.C., Cerdà, A., 2017. Ecosystem responses to land abandonment in Western Mediterranean Mountains. Catena 149 (Part3), 824–835. https://doi.org/10.1016/j.catena.2016.08.013.

Salvati, L., 2014. Agro-forest landscape and the 'fringe' city: a multivariate assessment of land-use changes in a sprawling region and implications for planning. Sci. Total Environ. 490, 715–723. https://doi.org/10.1016/j.scitotenv.2014.05.080.

Sánchez-Galiano, J.C., Martí-Ciriquián, P., Fernández-Aracil, P., 2017. Temporary population estimates of mass tourism destinations: the case of Benidorm. Tour. Manag. 62, 234–240.

SCS, 1986. Urban hydrology for small watersheds. In: SCSEDUSDOAT (Ed.), Release-55 164 pp.

Senciales-González, J.M., Rodrigo-Comino, J., Smith, P., 2020. Surveying topographical changes and climate variations to detect the urban heat island in the city of Málaga (Spain). Cuad. Investig. Geogr. 46, 521–543. https://doi.org/10.18172/cig.4228.

Senent-Aparicio, J., Alcalá, F.J., Liu, S., Jimeno-Sáez, P., 2020. Coupling SWAT model and CMB method for modeling of high-permeability bedrock basins receiving interbasin groundwater flow. Water 12, 1–19.

Slack, R.B., Welch, R., 1980. Soil conservation service runoff curve number estimates from landsat data. J. Am. Water Resour. Assoc. 16 (5), 887–893.

Sneyers, R., 1992. On the use of statistical analysis for the objective determination of climatic change. Meteorol. Z. 1, 247–256. https://doi.org/10.1127/metz/1/1992/247.

Sraj, M., Dirnbek, L., Brilly, M., 2010. The influence of effective rainfall on modeled runoff hydrograph. J. Hydrol. Hydromech. 58 (1), 3–14.

Tarboton, D.G., Bras, R.L., Rodriguez-Iturbe, I., 1991. On the extraction of channel networks from digital elevation data. Hydrol. Process. 5, 81–100.

Tohuami, I., Andreu-Rodes, J.M., Chirino, E., Sánchez, J.R., Moutahir, H., Pulido-Bosch, A., 2013. Recharge estimation of a small karstic aquifer in a semi-arid Mediterranean region (southeastern Spain) using a hydrological model. Hydrol. Process. 27, 165–174.

Valdes-Abellan, J., Pardo, M.A., Jodar-Abellan, A., Pla, C., Fernandez-Mejuto, M., 2020. Climate change impact on karstic aquifer hydrodynamics in southern Europe semi-arid region using the KAGIS model. Sci. Total Environ. 723, 138110.

Valdes-Abellan, J., Pardo, M.A., Tenza-Abril, A.J., 2017. Observed precipitation trend changes in the western Mediterranean region. Int. J. Climatol. 37, 1285–1296. https://doi.org/10.1002/joc.4984.

Valdes-Abellan, J., Pla, C., Fernandez-Mejuto, M., Andreu, J.M., 2018. Validating the KAGIS black-box GIS-based model in a Mediterranean karst aquifer: case of study of mela aquifer (SE Spain). Hydrol. Process. 32, 2584–2596. https://doi.org/10.1002/hyp.13215.

Xueqin, W., Qiqing, Y., 2005. Unbiasedness of the theil-sen estimator. J. Nonparametr. Stat. 17 (6), 685–695. https://doi.org/10.1080/10485250500039452.

Zeraatpisheh, M., Bakhshandeh, E., Hosseini, M., Alavi, S.M., 2020. Assessing the effects of deforestation and intensive agriculture on the soil quality through digital soil mapping. Geoderma 363, 114139. https://doi.org/10.1016/j.geoderma.2019.114139.